Projections of Exceptional Climatic Events in South East Queensland Produced by a Dynamical Regional Circulation Model

David Kent, Wenju Cai and Kim Nguyen

May 2012

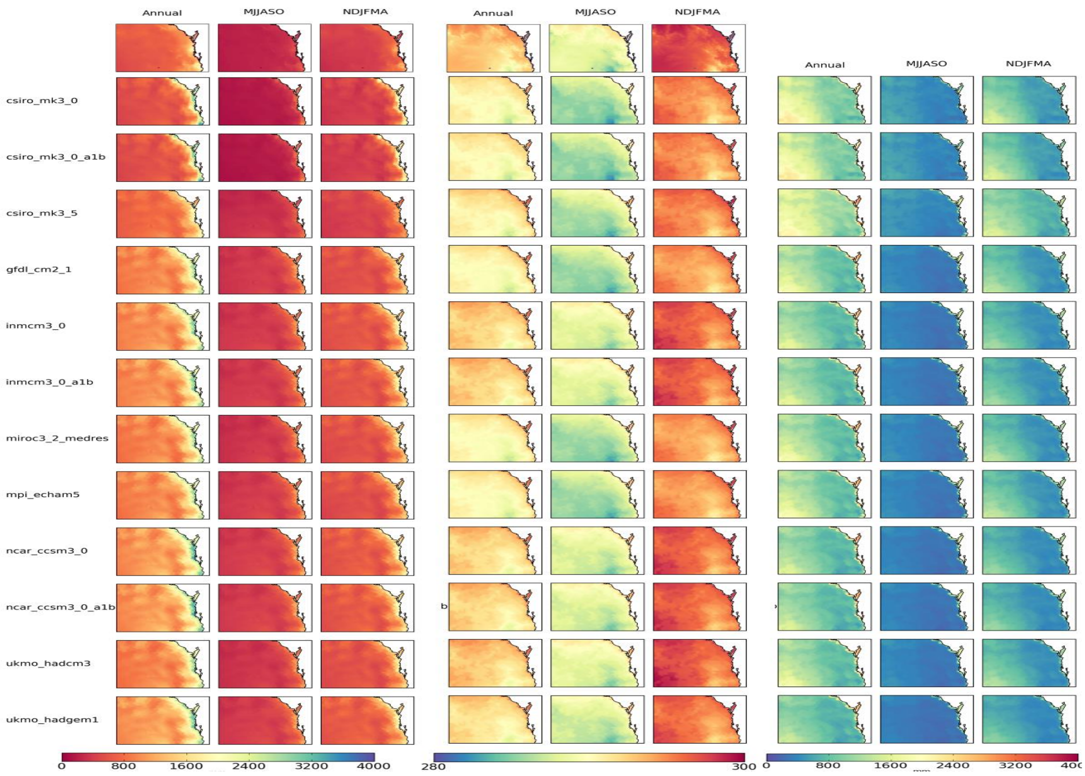

Urban Water Security Research Alliance
Technical Report No. 62

Queensland Government
National Research FLAGSHIPS Water for a Healthy Country
CSIRO
Griffith UNIVERSITY
THE UNIVERSITY OF QUEENSLAND AUSTRALIA

Urban Water Security Research Alliance Technical Report ISSN 1836-5566 (Online)
Urban Water Security Research Alliance Technical Report ISSN 1836-5558 (Print)

The Urban Water Security Research Alliance (UWSRA) is a $50 million partnership over five years between the Queensland Government, CSIRO's Water for a Healthy Country Flagship, Griffith University and The University of Queensland. The Alliance has been formed to address South East Queensland's emerging urban water issues with a focus on water security and recycling. The program will bring new research capacity to South East Queensland tailored to tackling existing and anticipated future issues to inform the implementation of the Water Strategy.

For more information about the:

UWSRA - visit http://www.urbanwateralliance.org.au/
Queensland Government - visit http://www.qld.gov.au/
Water for a Healthy Country Flagship - visit www.csiro.au/org/HealthyCountry.html
The University of Queensland - visit http://www.uq.edu.au/
Griffith University - visit http://www.griffith.edu.au/

Enquiries should be addressed to:

The Urban Water Security Research Alliance
PO Box 15087
CITY EAST QLD 4002

Ph: 07-3247 3005
Email: Sharon.Wakem@qwc.qld.gov.au

Project Leader – Wenju Cai
CSIRO Marine and Atmospheric Research
ASPENDALE VIC 3195

Ph: 03-9239 4419
Email: Wenju.Cai@csiro.au

Authors: CSIRO

Kent, D., Cai, W. and Nguyen, K. (2012). *Projections of Exceptional Climatic Events in South East Queensland Produced by a Dynamical Regional Circulation Model*. Urban Water Security Research Alliance Technical Report No. 62.

Copyright

Disclaimer

Cover Photograph:

Description: Historical climatology graphs.
© CSIRO

ACKNOWLEDGEMENTS

This research was undertaken as part of the South East Queensland Urban Water Security Research Alliance, a scientific collaboration between the Queensland Government, CSIRO, The University of Queensland and Griffith University.

Particular thanks go to members of the Project Reference Panel for their guidance in undertaking the Climate and Water research project for the Alliance, in particular David Robinson, Jozef Syktus and Ken Day (QCCCE); John Ruffini (DSITIA); Patricia Hurikino and Wai-Tong Wong (QWC); and Ryan McAllister (CSIRO).

FOREWORD

Water is fundamental to our quality of life, to economic growth and to the environment. With its booming economy and growing population, Australia's South East Queensland (SEQ) region faces increasing pressure on its water resources. These pressures are compounded by the impact of climate variability and accelerating climate change.

The Urban Water Security Research Alliance, through targeted, multidisciplinary research initiatives, has been formed to address the region's emerging urban water issues.

As the largest regionally focused urban water research program in Australia, the Alliance is focused on water security and recycling, but will align research where appropriate with other water research programs such as those of other SEQ water agencies, CSIRO's Water for a Healthy Country National Research Flagship, Water Quality Research Australia, eWater CRC and the Water Services Association of Australia (WSAA).

The Alliance is a partnership between the Queensland Government, CSIRO's Water for a Healthy Country National Research Flagship, The University of Queensland and Griffith University. It brings new research capacity to SEQ, tailored to tackling existing and anticipated future risks, assumptions and uncertainties facing water supply strategy. It is a $50 million partnership over five years.

Alliance research is examining fundamental issues necessary to deliver the region's water needs, including:

- ensuring the reliability and safety of recycled water systems.
- advising on infrastructure and technology for the recycling of wastewater and stormwater.
- building scientific knowledge into the management of health and safety risks in the water supply system.
- increasing community confidence in the future of water supply.

This report is part of a series summarising the output from the Urban Water Security Research Alliance. All reports and additional information about the Alliance can be found at http://www.urbanwateralliance.org.au/about.html.

Chris Davis
Chair, Urban Water Security Research Alliance

CONTENTS

LIST OF FIGURES

EXECUTIVE SUMMARY

There is strong demand for projections of changes in exceptional drought and rainfall events in order to inform policy in fields such as water management, agriculture and urban development. In an attempt to provide some guidance, twelve dynamical downscaling simulations have been performed using the CSIRO Conformal-cubic Atmospheric Model (CCAM) for the South East Queensland (SEQ) region. Changes in exceptional rainfall, temperature and evaporation events have been projected. In addition, a drought index was derived from these data using a modified Palmer Drought Severity Index (PDSI).

The twelve downscaling experiments project a hotter, more drought-prone SEQ region. These changes appear to be driven primarily by local warming and the associated increase in evaporative potential and not by any clear signal in rainfall.

The research shows that trends in rainfall have little impact on the mean or variability of the PDSI, while the strong positive trend in potential evaporation moves the PDSI into a persistently negative state. This indicates a transition into a state where evaporation potential is much greater than the available water over the 21st century.

In order to assess the impact of spatial resolution on the projected change in water availability, two additional CCAM runs were completed, one at eight kilometre (km) resolution and one at 20 km, using identical model configurations and external forcing. The evaluation of the modelled climatologies and variability demonstrated that the primary benefit of this increase of resolution (both from the broad scale GCMs to 20 km and from 20 km to 8 km) appears to be the improved simulation of inter-year rainfall variability rather than the rainfall climatology.

1. INTRODUCTION

The duration, frequency and intensity of periods of exceptionally dry or exceptionally wet conditions are key inputs to urban infrastructure planning. These characteristics of exceptional events are unlikely to be stationary over the coming century. As such, there is strong demand for projected changes in exceptional events in order to inform policy in fields such as water management, agriculture and urban development. This study uses a high spatial resolution regional circulation model (RCM) to produce such projections for South East Queensland (SEQ).

Twelve dynamical downscaling simulations have been performed using the CSIRO Conformal-cubic Atmospheric Model (CCAM) at a resolution of 20km. Each simulation was forced by the sea surface temperature (SST) fields produced by one of the Global Circulation Models (GCMs) submitted to the World Climate Research Program's (WCRP) Coupled Model Intercomparison Project phase 3 (CMIP3) multi-model dataset. In each case, the SST fields were bias corrected before they were used to force CCAM, see McGregor and Nguyen (2009) for more on this process. The downscaling process saves output for a comprehensive range of variables on a sub-daily time-scale and at a resolution of around 20km over much of eastern Australia. Rainfall, temperature and pan evaporation fields for a region bounded by 20–29°S and 145–155°E are extracted from this dataset and analysed.

In addition, a drought index is derived from these data. The index used is a modified Palmer Drought Severity Index (PDSI) (Palmer, 1965). The PDSI is based on a simple two-level soil moisture water-balance model. The original index published by Palmer made use of the estimation of potential evaporation by Thornthwaite (1948), but this simple approximation (based only on latitude and temperature) has been shown not to replicate observed trends in pan evaporation (Hobbins *et al.*, 2008). To overcome this issue, the pan evaporation from the RCM was used directly in the PDSI calculation.

In order to investigate the impact of increased resolution on water availability projections, two additional runs with the same external forcing and model configuration, but using different spatial resolutions, were completed. These were forced by the bias-corrected SST of the GFDL-CM2.1 model and use resolutions of 20 km and 8 km. They are discussed in Section 4.

2. HISTORICAL CLIMATOLOGY

Figure 1 shows the annual, dry half-year (May to October, labelled MJJASO) and wet half-year (November to April, labelled NDJFMA) mean rainfall (left), temperature (centre) and potential evaporation (right) for the period 1971-2000.

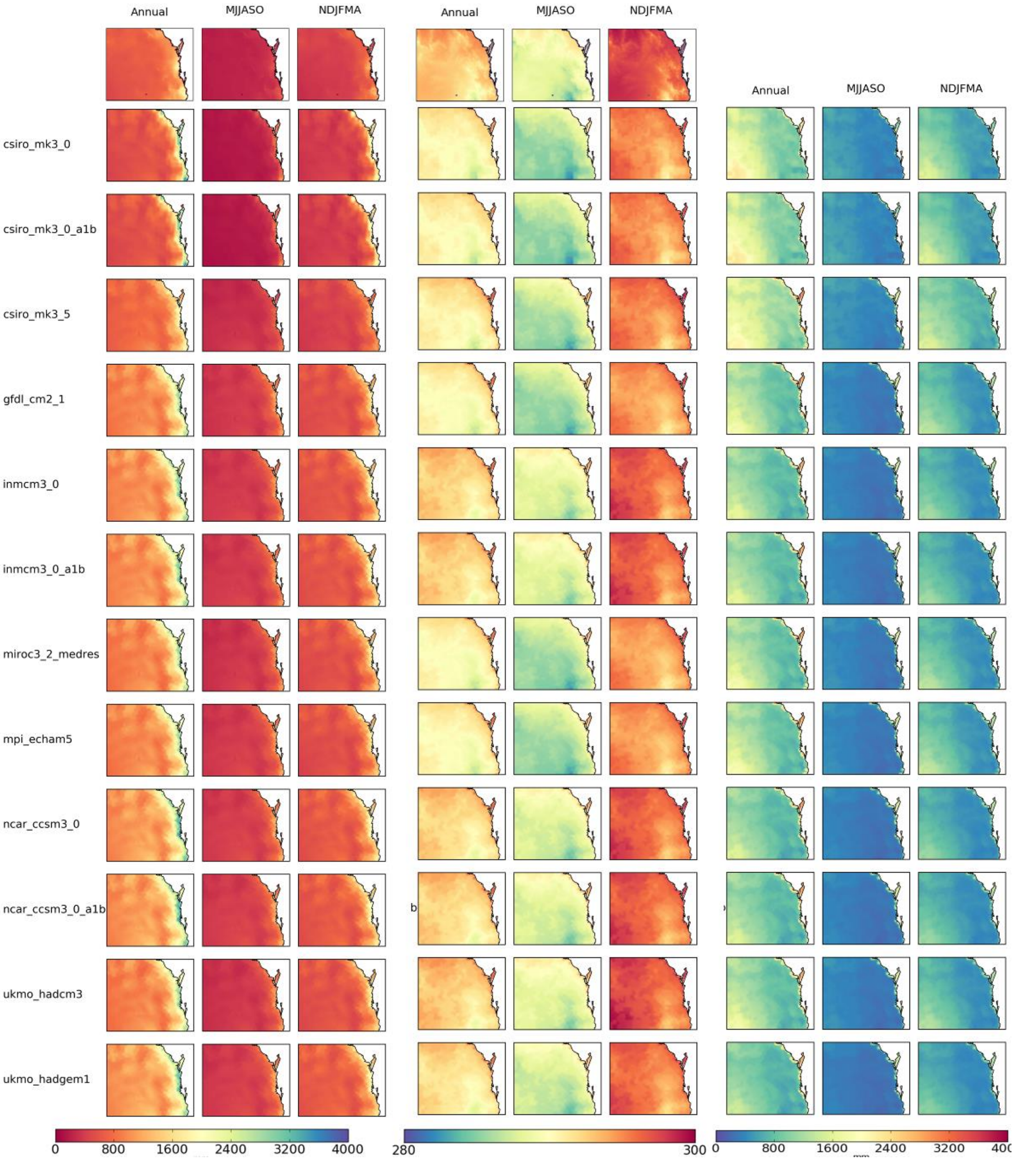

Figure 1. Annual, wet half-year (May to October, MJJASO) and dry half-year (November to April, NDJFMA) climatology for rainfall (left), temperature (centre) and potential evaporation (right). Top row is the observed, the remainder are CCAM results. All for 1971-2000 period.

The top row shows the observed values and the other rows show one CCAM simulation each. The rainfall distribution shows high coastal values, particularly in the wet-half year. The modelled results show greater rainfall than observed along the coast with a range of magnitudes across the models. There appears to be much more rainfall on the northern section of the coast than is observed.

The inter-model variation in average temperature is more pronounced. However, the modelled temperature distribution captures the much cooler, higher altitude areas in the south along with strong seasonal differences. Potential evaporation shows a strong coastal influence and with high potential there and in the inland regions.

Figure 2 gives a quantitative comparison of the observed and modelled spatial fields of climatological rainfall (top) and rainfall variability (bottom). The metric presented is the Watterson (2008) M-statistic which assesses the similarity of two spatial fields, with 1.0 indicating a good match and lower numbers a lower degree of similarity. Figure 2 presents this metric for all the CCAM runs as well as for each of the GCMs in the CMIP3 archive.

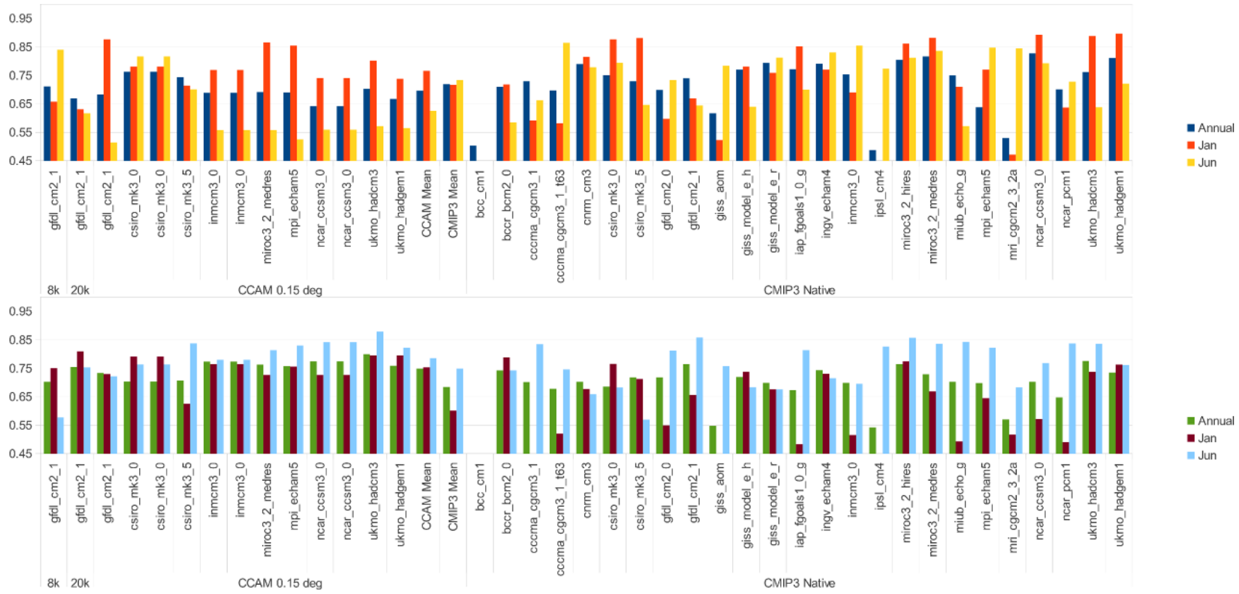

Figure 2. Watterson M-statistic for spatial distribution of climatological rainfall (top) and rainfall inter-year variability (bottom) compared to AWAP for the Moreton catchment area.

In general, there is little difference between the climatological performance of CCAM and the broad scale CMIP3 models, with both models comparably representing the spatial pattern of rainfall (dominated by a gradient from the coast) at a resolution of around 20 km. However, the inter-year variability is much better resolved by CCAM than it is by most of the GCMs (although some do score relatively well). Given the variability between individual CCAM runs, it is difficult to determine whether the higher-resolution 8 km run has any impact on this representation.

3. PROJECTED CHANGE IN EXCEPTIONAL EVENTS

In order to assess changes in the duration and frequency of exceptionally wet and dry periods, we present exceptional event characteristics in three ways: a time-series of the areal mean PDSI; analysing the proportion of SEQ experiencing a long-term shift in the incidence of exceptional events; and examining changes in the number and duration of events.

Figure 3 (following) shows the monthly progression of the PDSI over time for each of the twelve simulations, the bold line is the decadal average. A value less than zero indicates a water-deficiency, with severe drought events highlighted in colour (three – five months in yellow, six – 11 months in orange and 12 months or greater in red). All simulations show a high degree of variability on the annual to five-year time-scale, with regular periods of water deficit and excess. However, at least half of the simulations show an increase in periods of water deficit from the 2050s onward. The reasons for this can be determined by examining changes in exceptional rainfall, temperature and evaporation events. To do so we use a definition of exceptional events similar to that of Hennessy *et al*. (2008). Any value that falls outside the fifth percentile of the reference period (1971-2000) is considered to be exceptional. For example, a value lower than the fifth percentile rainfall for a location is an exceptionally dry value for that location, while a value greater than the 95th percentile is considered exceptionally wet.

Figures 4 and 5 (following) show 30-year running mean values of the percentage of the SEQ area experiencing exceptional events for each variable to 2080. Figure 4 shows all the hotter, drier extremes. The proportion of SEQ experiencing exceptionally low rainfall (top), high temperatures (second row), high pan evaporation (third row) and severely negative PDSI (bottom) is shown in Figure 4. The shaded area represents the 10th to 90th percentile range of the 12 downscaling simulations, with the bold line showing the median. The left column shows the full year, the middle column the dry-half year (May - October) and the right shows the wet half-year (November - April). The simulations exhibit strong increases in the proportion of SEQ experiencing exceptionally hot conditions to 2080, with more rapid changes over the dry half-year than the wet.

There is a similar increase in the incidence of potential evaporation extremes and in the proportional area experiencing severe water balance deficit. However, there is little to no trend in the proportional area simulated to experience exceptionally dry conditions, particularly over the wet season. There is more uncertainty in the proportion of SEQ experiencing exceptionally negative PDSI values. The lower end of the simulations suggest little change while the upper end shows up to 40% of SEQ experiencing frequent severe events.

At the other end of the spectrum, Figure 5 shows the cooler, wetter extremes. The 30-year running mean of the proportion of SEQ experiencing exceptionally high rainfall is shown in the top row, low temperatures (second row), low pan evaporation (third row) and greatly positive PDSI (bottom row).

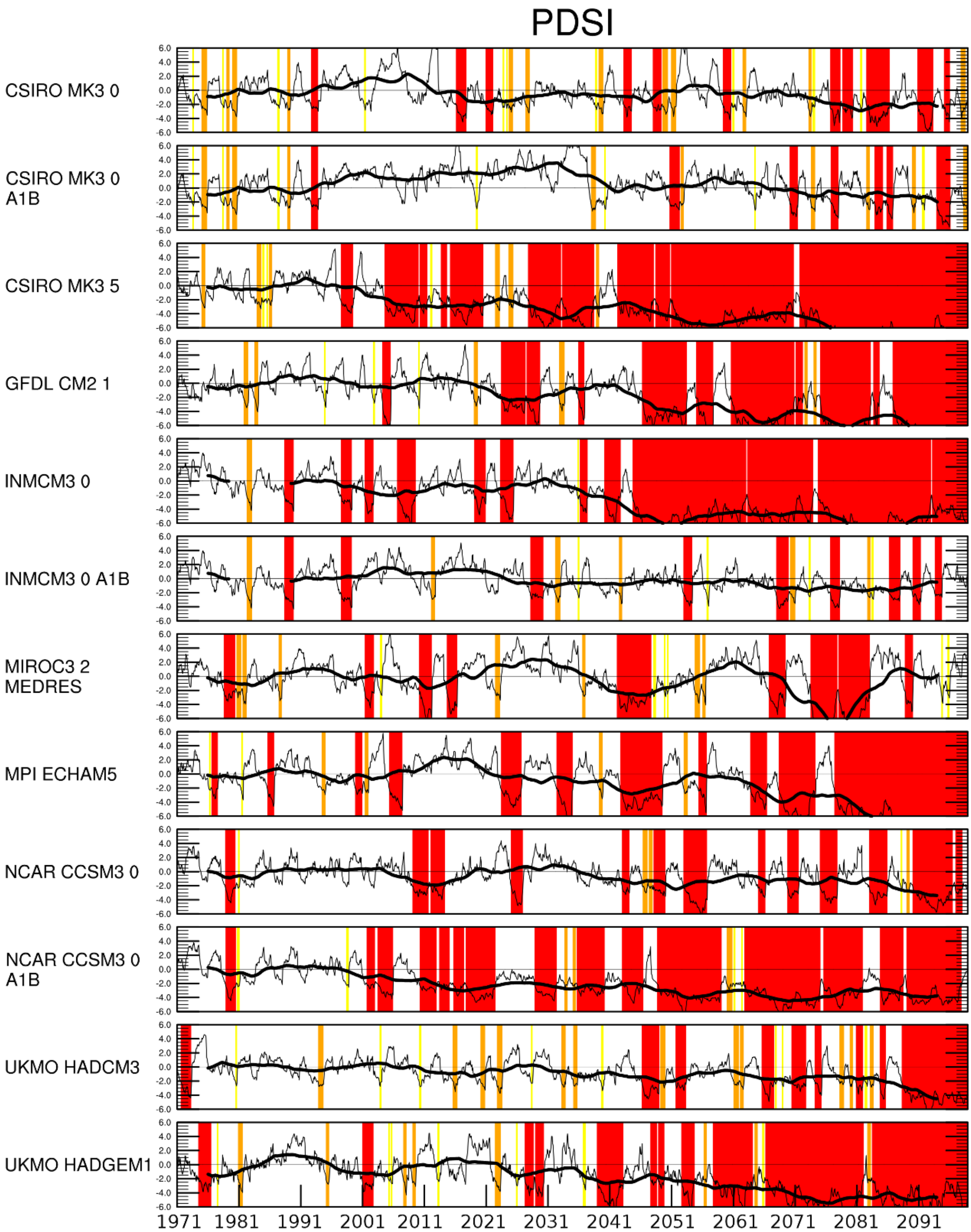

Figure 3. **PDSI time-series for each simulation.**

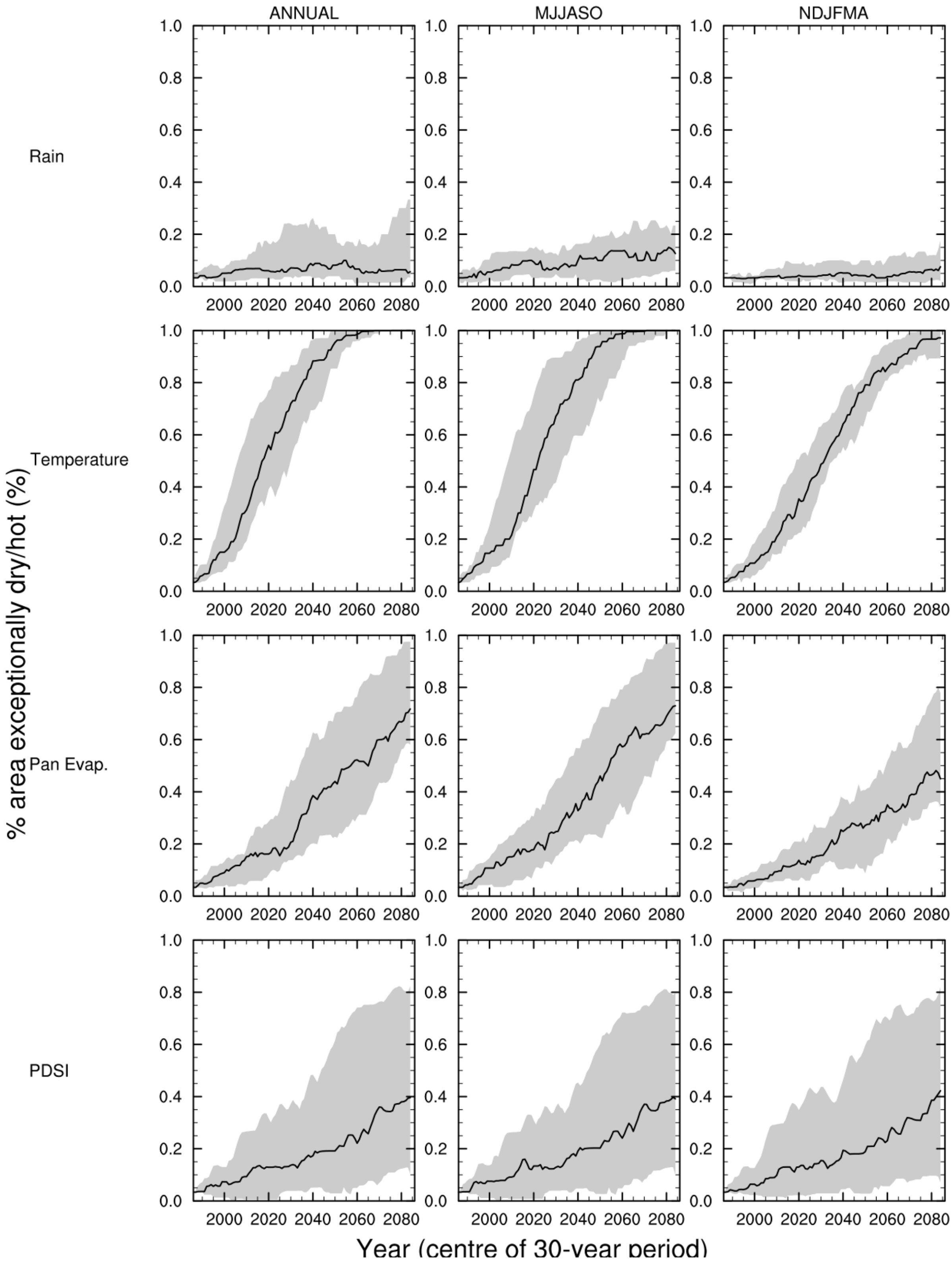

Figure 4. 30-year running mean time series of the percentage of SEQ experiencing exceptionally dry (top), hot (second row), high evaporation potential (third row) and severe drought (bottom) years (left), wet half-years (centre) and dry half-years (right).

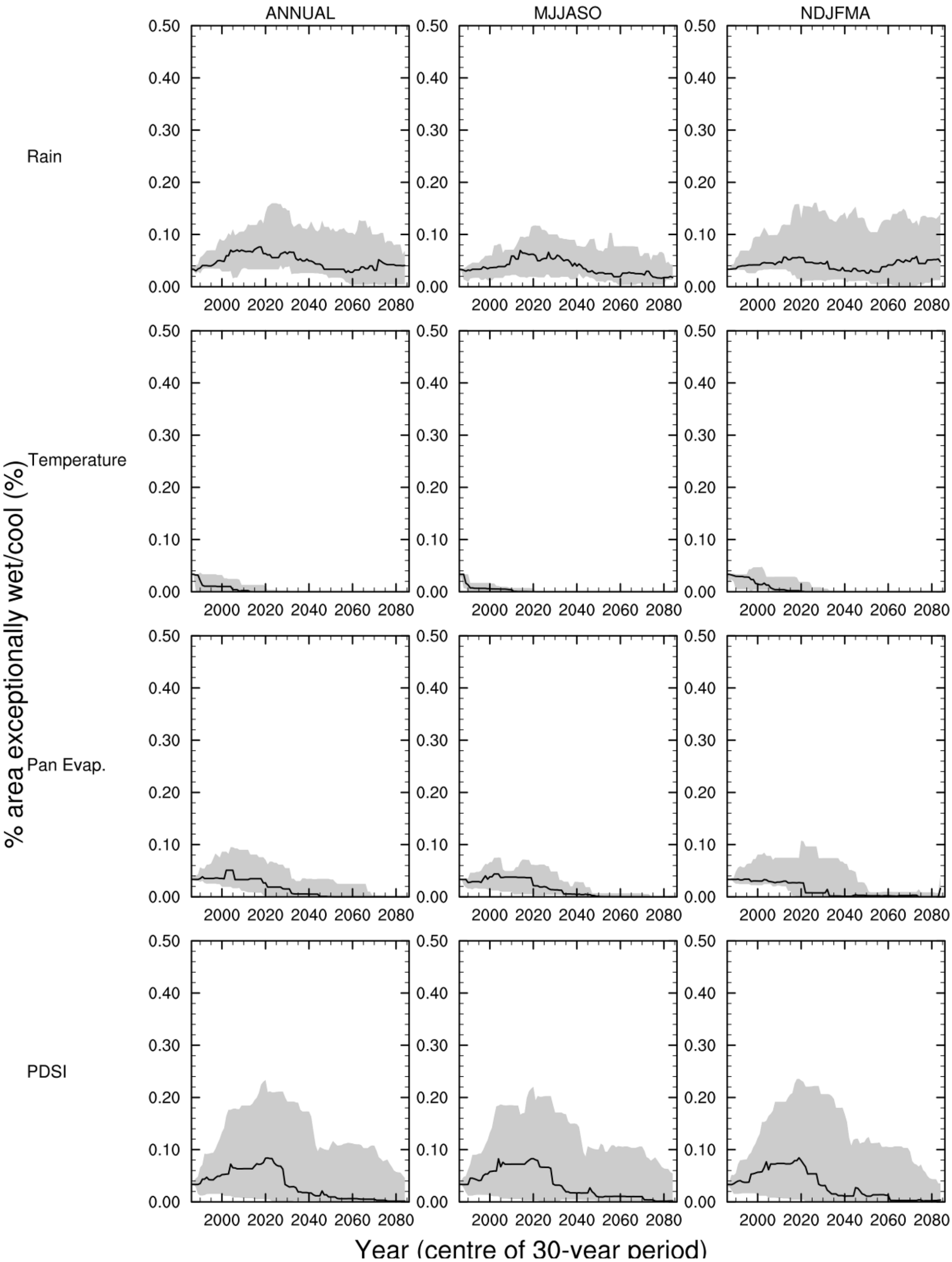

Figure 5. 30-year running mean time series of the percentage of SEQ experiencing exceptionally wet (top), cool (second row), low evaporation potential (third row) and unusually wet (bottom) years (left), wet half-years (centre) and dry half-years (right).

Once again, the proportion of SEQ experiencing exceptional rainfall events shows little change over the twenty-first century, suggesting that the frequency of periods of successive wet years (and half-years) are unlikely to change. All of the simulations show an absence of cold periods and suggest that by 2050 the occurrence of periods of low evaporation will reduce.

The analysis presented above is limited to describing changes to a climatology of exceptional events. In order to examine plausible changes in the incidence of exceptional events, we need to examine the number and duration of events in each simulation. The left panel of Figure 6 shows the number of exceptionally low PDSI (severe moisture deficit) events for five 30-year periods (centred on 1985, 2010, 2035, 2060, 2085). An event is diagnosed as a period of a year or more when more than 20% of SEQ experiences a severe moisture deficit. The black line shows the median of the twelve simulations, with the shaded area representing the 10th to 90th percentile of the simulations. The number of events is shown to increase from an average of around one event in the current period to three events at the end of the 21st century. The right-hand panel shows the mean duration of events over the same time periods. It also shows an increase across the 21st century, from a mean duration of one year per event to a mean duration of ten years. There is a large spread of results across the simulations for both metrics, with changes in the mean duration ranging from one year to twenty years by the 2085 period.

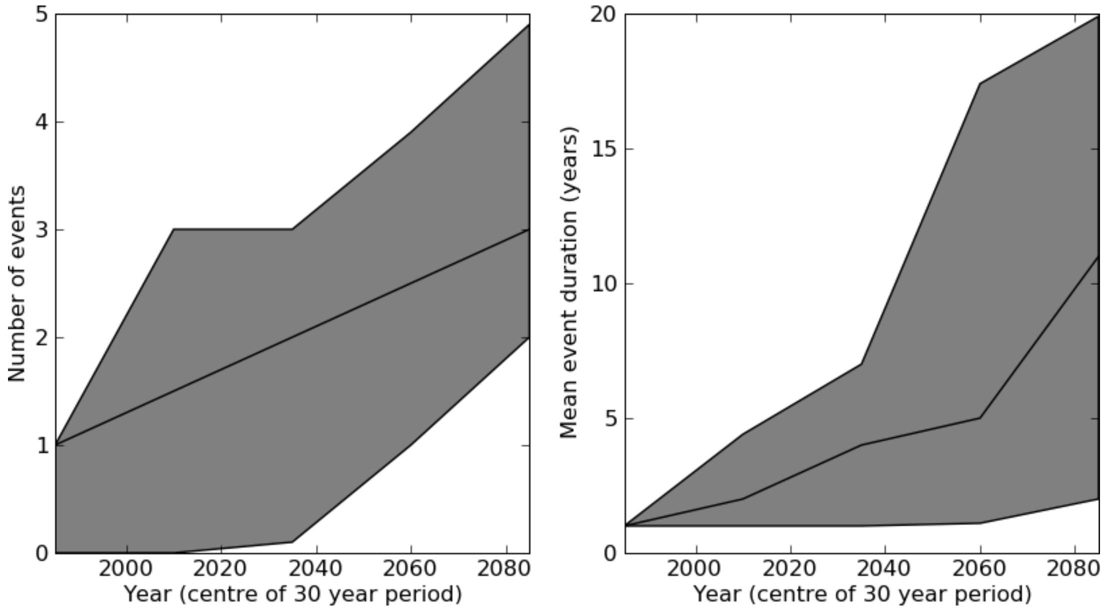

Figure 6. The frequency (left) and mean duration (right) of exceptionally negative PDSI events at five 30-year time periods. Black line shows multi-model median and the shaded area indicates the 10th to 90th percentile range.

4. DISCUSSION AND CONCLUSIONS

The twelve downscaling experiments project a hotter, more drought-prone SEQ. These changes appear to be driven primarily by a local warming and associated increase in evaporative potential and not by any clear signal in rainfall. As a test of this hypothesis, the PDSI calculation has been rerun for a number of the simulations under two sets of conditions. Firstly, all potential evaporation values are set to a mean 1971-2000 monthly climatology, removing its trend from the calculation. Secondly, rainfall is constrained to its 1971-2000 climatology. Figure 7 (following) shows the areal-mean (over SEQ) time-series of PDSI for both tests (original time-series at top, climatological potential evaporation middle and climatological rainfall at the bottom) for three of the downscaling simulations: a low simulation MIROC3.2-MEDRES; medium simulation MPI/ECHAM5; and a dry simulation CSIRO Mk3.5. The figure shows that trends in rainfall have little impact on the mean or variability of the PDSI while the strong positive trend in potential evaporation moves the PDSI into a persistently negative state. This indicates a transition into a state where evaporation potential is much greater than the available water over the 21st century.

In order to assess the impact of spatial resolution on the projected change in water availability two additional CCAM runs were completed, one at 8km resolution and one at 20km. Both runs used identical model configurations and external forcing. Figure 8 (following) shows the projected change in rainfall and temperature for each month for both runs over the 21st century. Broadly speaking there are no major differences in the projections of the two runs and the differences that do exist are likely to be within the bounds of the natural variability of the model (as suggested by the 12 member 20km ensemble). Over the Moreton Bay catchment, the 20 km run projects a change of -2.79 mm per day per degree of global temperature increase for annual rainfall, while the 8km run projects -4.85 mm per day per degree warming. The changes in temperature are 1.08 and 1.26 degrees. The evaluation of the modelled climatologies and variability in Section 2 demonstrated that the primary benefit of this increase of resolution (both from the broad scale GCMs to 20km and from 20km to 8km) appears to be the improved simulation of inter-year rainfall variability rather than the rainfall climatology.

There are a number of issues that must be considered when interpreting these findings. It should be noted that the results presented here are produced by only one atmospheric model (albeit forced by twelve different SST patterns), with no assessment of the sensitivity of this model to changes and variability in the driving SST patterns. This study does not make any assessment of the atmospheric processes driving rainfall, temperature and pan evaporation over SEQ. We assume that because the regional circulation model (RCM) replicates most of the observed features of these fields it does so as a result of the right processes. In particular, further work is needed to examine how the RCM responds to large-scale modes of variability such as the El Nino Southern Oscillation, which strongly influences SEQ rainfall variability.

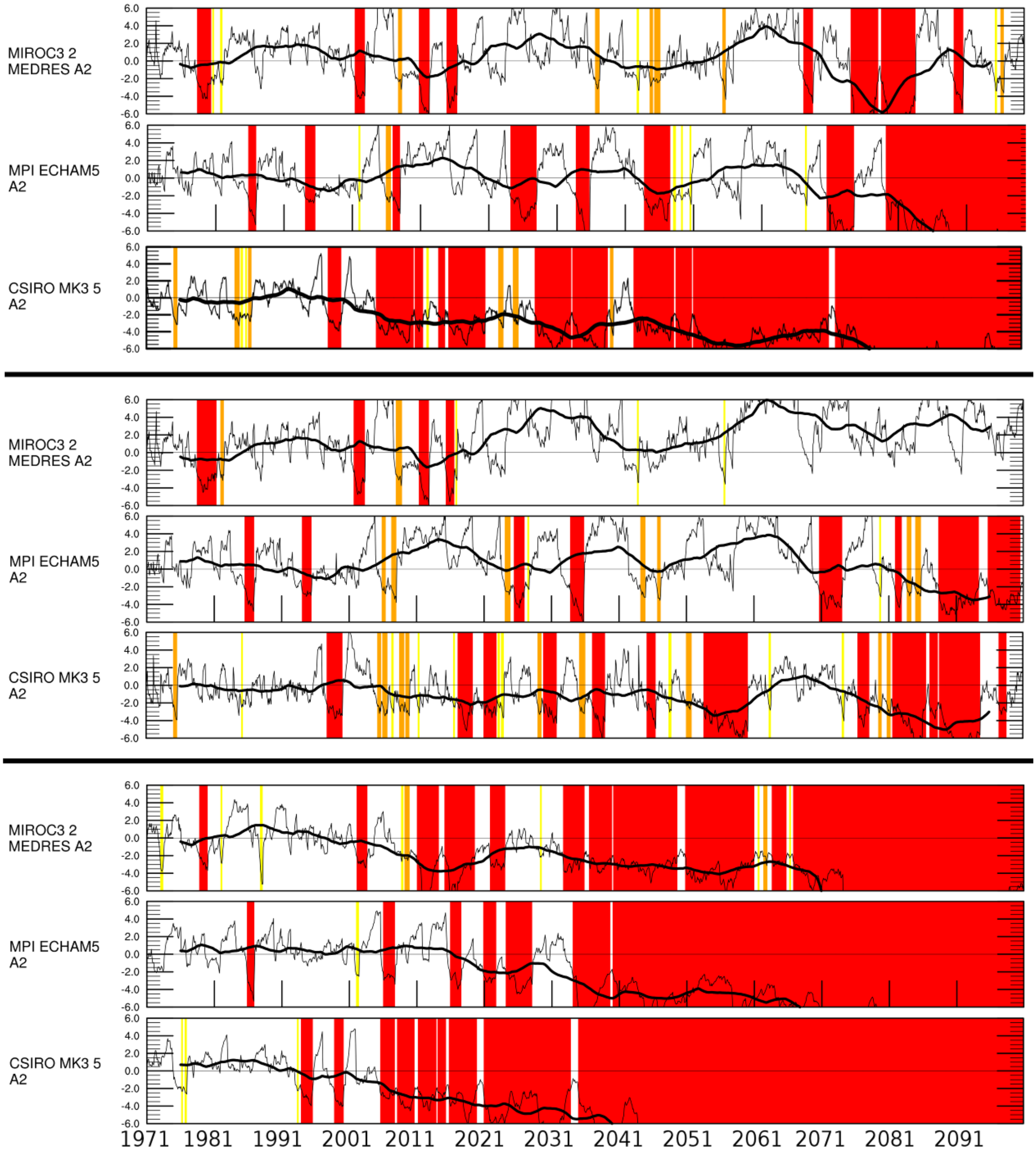

Figure 7. **PDSI time-series for the three of the 12 simulations (spanning the range of results). Original calculation (top), using climatological potential evaporation (middle) and using climatological rainfall (bottom).**

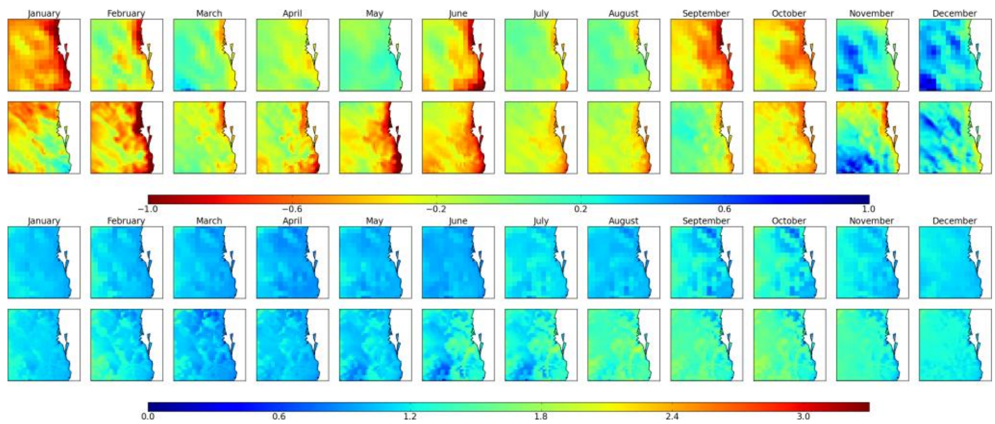

Figure 8. **Monthly projected change in rainfall (mm per day per degree global temperature increase) from the 20km run (row 1) and 8km (row 2) runs and projected change in temperature (degree per degree global temperature increase) from the 8 km (row 3) and 20km (row 4).**

REFERENCES

Hennessy, K., R. Fawcett, D. Kirono, F. Mpelasoka, D. Jones, J. Bathols, P. Whetton, M. Stafford Smith, M. Howden, C. Mitchell, and N. Plummer, 2008, *An assessment of the impact of climate change on the nature and frequency of exceptional climatic events*, Tech. rep., CSIRO and Bureau of Meteorology.

Hobbins, M. T., A. Dai, M. L. Roderick, and G. D. Farquhar, 2008, *Revisiting the parameterization of potential evaporation as a driver of long-term water balance trends*, Geophysical Research Letters, 35, L12,403, 10.1029/2008GL033840.

McGregor, J., and K. Nguyen, 2009, *Dynamical downscaling from climate change experiments*, Tech. rep., South Eastern Australian Climate Initiative.

Palmer, W., 1965, *Meteorological drought, research paper no. 45*, Tech. rep., US Weather Bureau, Washington DC.

Thornthwaite, C., 1948, *An approach toward a rational classification of climate*, Geographical Review, 38, 55–94.

Watterson IG. 2008. *Calculation of probability density function for temperature and precipitation change under global warming.* Journal of Geophysical Research 113: D12106,doi:10.1029/2007JD009254.

Urban Water Security Research Alliance